



Research article

Unfolding of core nucleosomes by PARP-1 revealed by spFRET microscopy

Daniel Sultanov^{1,2}, Nadezhda Gerasimova¹, Kseniya Kudryashova^{1,3}, Natalya Maluchenko¹, Elena Kotova², Marie-France Langelier⁴, John Pascal⁴, Mikhail Kirpichnikov², Alexey Feofanov^{1,3*} and Vasily Studitsky^{1,2,*}

¹ Biology Faculty, Lomonosov Moscow State University, Moscow, 119992, Russia

² Fox Chase Cancer Center, Philadelphia, PA, 19111-2497, USA

³ Shemyakin-Ovchinnikov Institute of Bioorganic Chemistry of Russian Academy of Sciences, 117997 Moscow, Russia

⁴ Department of Biochemistry and Molecular Medicine, Université de Montréal, 2900 Boulevard, Edouard-Montpetit, Montréal, QC H3T 1J4, Canada

* **Correspondence:** Email: avfeofanov@yandex.ru, vasily.studitsky@fccc.edu;
Tel: +215-214-7134; Fax: +215-728-3574.

Abstract: DNA accessibility to various protein complexes is essential for various processes in the cell and is affected by nucleosome structure and dynamics. Protein factor PARP-1 (poly(ADP-ribose) polymerase 1) increases the accessibility of DNA in chromatin to repair proteins and transcriptional machinery, but the mechanism and extent of this chromatin reorganization are unknown. Here we report on the effects of PARP-1 on single nucleosomes revealed by spFRET (single-particle Förster Resonance Energy Transfer) microscopy. PARP-1 binding to a double-strand break in the vicinity of a nucleosome results in a significant increase of the distance between the adjacent gyres of nucleosomal DNA. This partial uncoiling of the entire nucleosomal DNA occurs without apparent loss of histones and is reversed after poly(ADP)-ribosylation of PARP-1. Thus PARP-1-nucleosome interactions result in reversible, partial uncoiling of the entire nucleosomal DNA.

Keywords: PARP-1 protein; DNA repair; chromatin structure; nucleosome; DNA-histone interactions

1. Introduction

Eukaryotic genome is composed of nucleosomes that consist of 145–148 bp DNA segments wrapped around the histone octamer in 1.65–1.7 superhelical coils. Nucleosomal organization limits DNA accessibility to various proteins, including protein complexes involved in DNA repair [1]. Various protein complexes, including ATP-dependent chromatin remodelers and PARP-1 protein reorganize chromatin, making it more accessible to other DNA-interacting proteins.

PARP-1 is an abundant multi-domain protein, localized in cell nuclei of higher eukaryotes, with a range of diversity functions, playing role in DNA repair [2,3], chromatin organization and transcription [4]. One of the crucial roles of the protein in a cell is detection of DNA damages through its DNA-binding zinc-finger domains that recognize single- and double-strand DNA breaks [5]. A variety of factors (e.g., ionizing radiation) cause genome damage making double-strand breaks in DNA, which can lead to mutations. PARP-1 binding to a DNA strand break induces a conformational change in the protein [6,7], which results in its DNA-dependent activation and poly(ADP)-ribosylation (pADP-r) of the target proteins (including automodification of PARP-1) using NAD^+ as a substrate. Core histones [8] and linker histone H1 [9] are among the targets for pADP-r. Some direct inhibitors of PARP-1 enzymatic activity are important anticancer compounds. Thus anticancer compound olaparib interferes with essential nuclear processes in various tumors and causes cell death due to synthetic lethality [10,11].

Although PARP-1 can bind to intact nucleosomes and to a variety of nucleosome substrates through double-strand break in nucleosomal DNA with different affinities [12], it is unknown whether it affects the structure of the nucleosome core. Using a single-particle Forster resonance energy transfer (spFRET) approach [13-16], we report that PARP-1 causes a considerable nucleosome unfolding *in vitro* that can be almost completely reversed by its automodification.

2. Materials and Methods

2.1. Protein purification and DNA templates

Human recombinant PARP-1 was expressed in *E.coli* and purified as described [17].

Fluorescently labeled DNA templates used for nucleosome assembly were synthesized by PCR using modified nucleosome-positioning sequence s603-42 [18] as a template. The following oligonucleotides were used to introduce fluorescent labels in nucleosomal DNA:

for nucleosomes N13/91: forward – 5'-ACCCAGGGACTTGAAGTAATAAGGACGGAGGG CCT#CTTTCAACATCGAT-3' (T# refers to a nucleotide with a Cy3 label), reverse – 5'-CAAGCG ACACCGGCACTGGGCCCCGGTTCGCGCTCCCTCCTTCCGTGTGTTGTCGT*CTCT-3' (T* refers to a nucleotide with a Cy5 label). For nucleosomes N35/112: forward – 5'-AAGCGACACCG GCACTGGGCCCCGGTTCGCGCT#CCCGCCTTCCGTGTGTTGTCGTCTCTCGGGCGT-3', reverse – 5'-ACCCAGGGACTTGAAGTAATAAGGACGGAGGGCCTCTTTCAACATCGATGC ACGGT*GGTTAG; for N57/135: forward – 5'- ACACCGGCACTGGGCCCCGGTTCGCGCTCCC TCCTTCCGTGTGTTGTCGTCTCTCGGGCGTCTAAGTACGCT#TAGGC-3', reverse – 5'-ACCC CAGGGACTT*GAAGTAATAAG-3'.

2.2. Nucleosome assembly and purification

Nucleosomes were assembled using chicken donor chromatin without linker histone by salt dialysis as described [19]. The mononucleosomes were then gel-purified as described [20]. In-gel FRET analysis was performed using a Typhoon PhosphorImager. Fluorescence was excited in gel at 532 nm wavelength and recorded at 570–610 nm (for Cy3) and 650–700 nm (for Cy5) spectral regions.

2.3. spFRET measurements

Fluorescently labeled nucleosomes at 3 nM were incubated with 50 or 100 nM PARP-1 for 20 minutes in a buffer containing 20 mM Tris-HCl pH 7.9, 5 mM MgCl₂, 150 mM KCl and 0.15 mM ZnCl₂ at +25 °C in siliconized tubes. To induce poly(ADP)-ribosylation, nucleosomes were incubated with 50 nM PARP-1 for 20 min and further incubated with 2 or 4 μM NAD⁺ for 15 min. spFRET analysis was performed for 15 min using facilities and settings described previously [13]. spFRET measurements were repeated in at least two independent experiments. In each experiment, data from 700 to 7000 single nucleosomes were analyzed. Preservation of structures of nucleosomes and PARP-1-nucleosome complexes during the analysis was further verified by comparing the results of two consequent measurements.

Efficiency of FRET and its changes were characterized by calculating proximity ratio (E_{PR}) for each single nucleosome:

$$E_{PR} = (I_5 - 0.19 \times I_3) / (I_5 + 0.81 \times I_3) \quad (1),$$

where I_5 and I_3 are measured fluorescence intensities of Cy5 and Cy3, respectively, and factors 0.19 and 0.81 provide correction for the contribution of Cy3 fluorescence in the Cy5 detection channel (spectral cross-talk). E_{PR} values calculated for nucleosome samplings were presented as frequency distribution histograms and fitted by two Gaussians. Goodness of the fit (R^2) varied from 0.84 to 0.99.

3. Results

3.1. The experimental approach for analysis of PARP-1-dependent changes in nucleosome structure

To study the effect of PARP-1 on the nucleosomal structure, spFRET microscopy experiments were conducted using three mononucleosomal templates; each nucleosome was labeled with a single pair of Cy3 and Cy5 fluorophores (Figure 1A). These labels were introduced in DNA based on known crystal structure of a nucleosome [21] to obtain efficient FRET between them in assembled nucleosomes without interfering with DNA structure or contacts between the DNA and core histones [13-16]. Labels were positioned into different parts of nucleosomal DNA: at +13 (Cy3) and +91 (Cy5) base pairs, relatively to the entry of linker DNA into nucleosome core (referred to as N 13/91), at positions +35 and +112 (N 57/135) and at +57 and +135 (N 57/135). In the assembled nucleosome, these positions are localized near the entry point of DNA into the nucleosome, near a contact between H2A-H2B histone dimers and close to the exit of DNA from nucleosome, respectively (Figure 1A).

Nucleosome assembly was carried out using chicken chromatin as a donor of core histones and a short DNA fragment containing nucleosome positioning sequence 603 [22] and additional terminal 20 bp linker. This linker provided a DNA end (“dsDNA break”) for PARP-1 binding to the

nucleosome (Figure 1A); PARP-1 cannot bind to the other DNA end localized at the nucleosomal boundary [12,23]. Quality of the assembly was estimated by native PAGE; the expected changes of the FRET signal in the nucleosomes as compared with histone-free DNA were observed in the gel (Figure 1B). Single-particle FRET measurements were conducted using gel-purified nucleosomes in solution under microscope. The Cy3 label was excited with 514.5 nm laser wavelength in single nucleosomes or complexes when they diffused freely through a small focal volume [13] (Figure 1C), and fluorescence intensities of both Cy3 (donor) and Cy5 (acceptor) dyes were measured. Proximity of the labels in single nucleosomes was characterized by calculating of so-called proximity ratio (E_{PR}), and the frequency distribution of E_{PR} was plotted for each nucleosome sample. Absolute distances between labels were not calculated because of insufficient data about quantum yields and an instrumental factor.

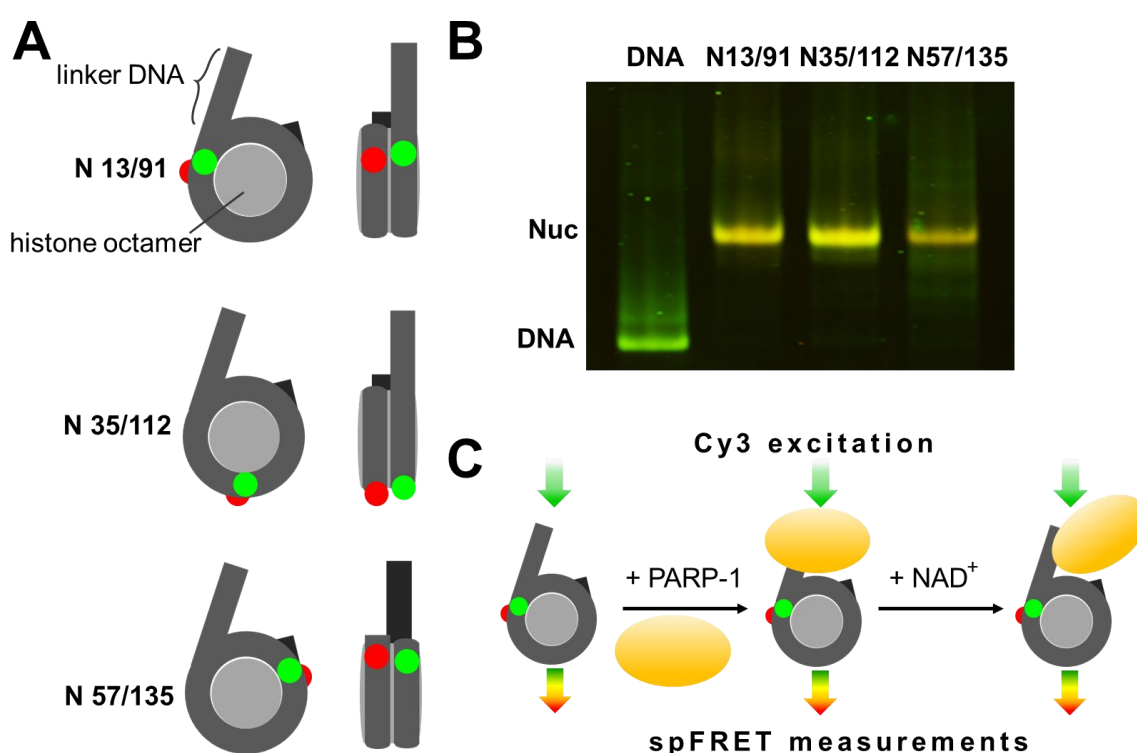


Figure 1. The experimental approach for analysis of PARP-1-dependent changes in nucleosome structure. **A.** Three types of mononucleosomes containing the single pair of Cy3 and Cy5 dyes in different positions on the nucleosomal DNA (the positions of Cy3 and Cy5 are shown by green and red circles, respectively). **B.** PAGE and in-gel FRET analysis of assembled nucleosomes and DNA template. Distributions of Cy3 and Cy5 fluorescence in a gel at a Cy3 excitation are shown in green and red, respectively. Yellow color (superposition of green and red colors) indicates a considerable FRET efficiency. **C.** Experimental approach. spFRET from nucleosomes was measured in the absence or presence of PARP-1 and subsequent addition of NAD⁺.

3.2. PARP-1 induces structural changes in nucleosomal DNA

In agreement with the previously published data [16], spFRET analysis revealed two populations of N 13/91 nucleosomes (Figure 2A, Table S1). A peak with the E_{PR} maximum at 0.69 corresponds to a major fraction of compact nucleosomes, while a peak with the E_{PR} maximum at 0.01 likely indicates the presence of a minor fraction of nucleosomes with partially unwrapped DNA. After addition of 50 nM PARP-1, the distribution of nucleosomes by E_{PR} is changed (Figure 2A) indicating formation of PARP-1-nucleosome complexes. These complexes are characterized by E_{PR} with a maximum at 0.31, while a shoulder in a higher E_{PR} region corresponds to PARP-1-free, more compact intact nucleosomes. Incomplete PARP-1 binding is observed most likely because the dissociation constant for PARP-1 complexes with similar nucleosome constructs is 85 nM [12]. In agreement with this proposal, a high E_{PR} shoulder disappears after increasing concentration of PARP-1 to 100 nM (Figure 2A). The low- E_{PR} peak at 0.01 is also diminished in the presence of PARP-1, suggesting that spontaneous DNA uncoiling from the octamer is diminished in the complex.

Domination of the single Gaussian peak in the frequency distribution of E_{PR} indicates formation of a single uniform population of nucleosome complexes with PARP-1. A shift of E_{PR} maximum from 0.69 to 0.31 shows that PARP-1 binding causes structural changes in nucleosomal DNA near the entrance of DNA into nucleosome, namely in the region, where DNA interacts with the H2A-H2B dimer (position +13) and H4-H2B interface (position +91). To evaluate a possibility that PARP-1 disrupts nucleosomes and forms complexes with histone-free DNA, the same experiments were conducted with DNA template used for nucleosome assembly (Figure 2B). In more extended histone-free DNA, the Cy3 and Cy5 labels are positioned far from each other and no FRET occurs (maximum of E_{PR} is 0.01, Figure 2B, Table S1). The frequency distribution of E_{PR} , which is observed for the histone-free DNA, is minimally affected by PARP-1 (Figure 2B).

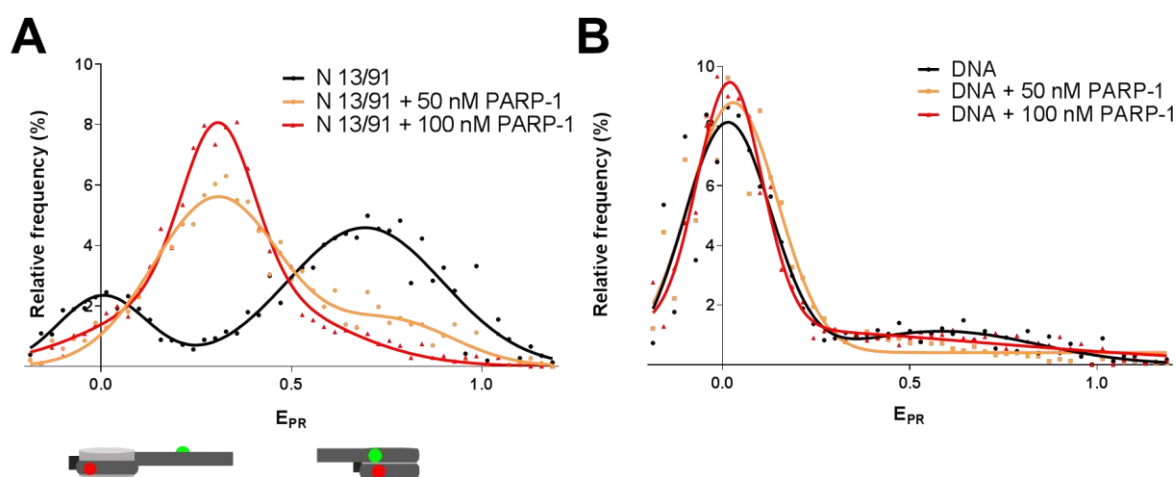


Figure 2. PARP-1 induces structural changes in nucleosomal DNA. **A.** spFRET analysis of PARP-1 binding to N 13/91 nucleosomes. Typical frequency distributions of E_{PR} are shown for N 13/91 nucleosomes before and after addition of 50 or 100 nM of PARP-1 (for quantitative and statistical data see Table S1). **B.** spFRET analysis of +13/+91-labeled DNA before and after addition of 50 or 100 nM of PARP-1.

In summary, binding PARP-1 to the N 13/91 nucleosome causes considerable structural changes in nucleosomal DNA that are accompanied by an increase in the distance between the labels introduced near the entrance of DNA into a nucleosome, indicating that gyres of nucleosomal DNA are coming apart and, at the same time, by diminished spontaneous DNA uncoiling from the octamer in the complex, suggesting that the DNA end has a lower mobility in the PARP-1-nucleosome complex. These observations, taken together, suggest that PARP-1 causes a mobility of the end of nucleosomal DNA, but, at the same time, induces uncoiling of nucleosomal DNA together with histones.

3.3. PARP-1 induces similar structural changes in different regions of nucleosomal DNA

To evaluate how PARP-1 affects other parts of nucleosomal DNA, N 35/112 and N 57/135 nucleosomes were analyzed (Figure 3). The N 13/91 (Figure 2A) and N 35/112 nucleosomes (Figure 3A) are characterized by similar frequency distributions of E_{PR} (see Table S1 for the statistical data). Although labels in the nucleosomes N 35/112 were positioned far from the extending DNA end (PARP-1 target), FRET between these labels was significantly affected by PARP-1 binding. The maximum of the main E_{PR} peak was shifted from 0.63 to 0.37, indicating to reorganization of nucleosomal DNA structure near the interface between the H2A/H2B dimers and H3/H4 tetramers (position +35) and/or H3/H4 tetramers (position +112) that resulted in the increase in the inter-label distance.

N 57/135 nucleosomes were also characterized by a bimodal distribution of E_{PR} (Figure 3B and Table S1). In the presence of 100 nM PARP-1, a broad E_{PR} distribution was formed with a maximum at 0.43. This broadening could be explained by an increased mobility of nucleosomal DNA localized near the position +135 in the PARP-1-nucleosome complex.

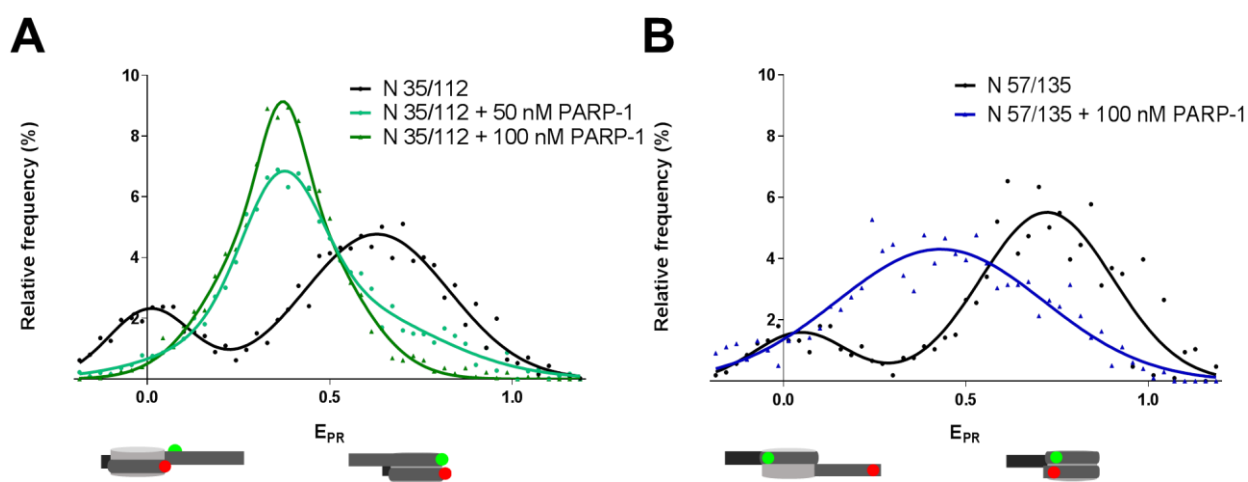


Figure 3. PARP-1 induces similar structural changes in different regions of nucleosomal DNA. spFRET analysis of PARP-1 binding to N 35/112 (A) and N 57/135 nucleosomes (B). Typical frequency distributions of E_{PR} are shown for nucleosomes before and after incubation in the presence of 50 or 100 nM of PARP-1 (for quantitative and statistical data see Table S1).

For every combination of the labels, the shift of the main peak from higher to intermediate E_{PR} values was observed. In the case of N 13/91 and N 35/112 the shift was accompanied by a significant decrease in the height of the low- E_{PR} peak (Figures 2 and 3). Taken together, the data indicate that PARP-1 can partially and similarly uncoil different regions of nucleosomal DNA, and, at the same time, can restrict mobilities of the +13, +35 and +112 regions of nucleosomal DNA.

3.4. PARP-1-induced changes in nucleosome structure are reversed after PARP-1 automodification

To elucidate how activation of the enzymatic activity of PARP-1 affects the structure of the PARP-1-nucleosome complex, pre-formed PARP-1 complexes with N 13/91 nucleosomes were incubated in the presence of different concentrations of NAD^+ . DNA-bound PARP-1 is activated, auto-poly(ADP)-ribosylated in the presence of NAD^+ and loses its capability to interact with damaged DNA and nucleosomes [23,24]. Therefore, it was expected that nucleosomal E_{PR} distribution would be recovered in the presence of NAD^+ . spFRET analysis revealed that incubation of the PARP-1-nucleosome complex in the presence of 2 or 4 μM NAD^+ results in a progressive, stepwise shift of the mean value of E_{PR} peak from 0.31 to 0.43 or to 0.62, respectively (Figure 4 and Table S1). In the presence of 4 μM NAD^+ , the main E_{PR} maximum (0.62) approaches the value, which is a characteristic of free nucleosomes (0.69), suggesting that nucleosome structure is almost completely recovered. Since the principal NAD^+ -dependent reaction is PARP-1 automodification [25], the data indicate that after partial automodification (i.e., at 2 μM NAD^+) PARP-1 remains bound to nucleosomes and forms a discrete intermediate PARP-1-nucleosome complex.

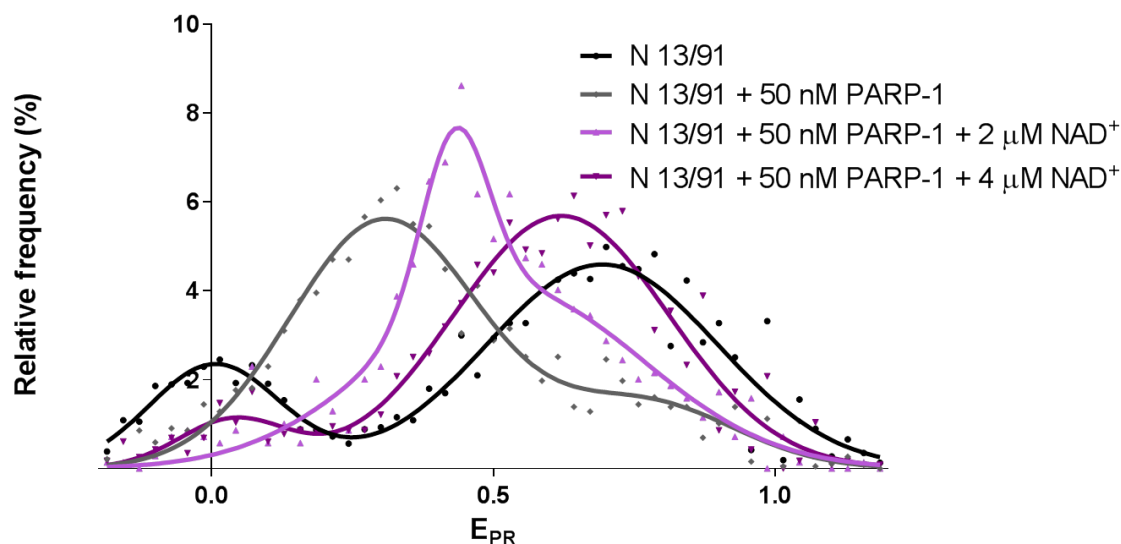


Figure 4. PARP-1-induced changes in nucleosome structure are reversed after PARP-1 automodification. spFRET analysis of PARP-1 automodification in the complex with nucleosomes N 13/91 after addition of NAD^+ . Typical frequency distributions of E_{PR} are shown (for quantitative and statistical data see Table S1).

Incomplete reversal of the nucleosomal E_{PR} distributions at 4 μM NAD^+ is likely explained by incomplete automodification of PARP-1 that remains bound to the nucleosome. Alternatively, poly(ADP)-ribosylation of core histones [8] prevents complete recovery of the nucleosomal structure.

4. Discussion

Our spFRET experiments suggest that PARP-1 binds to a nucleosome and induces disturbance of different regions of nucleosomal DNA: near the entrance/exit of DNA into/from a nucleosome, and in the region positioned ~ 35 bp from the boundaries of nucleosomal DNA (Figures 2 and 3). This uncoiling of nucleosomal DNA is accompanied by a reduced mobilities of the +13, +35 and +112 regions of nucleosomal DNA (Figures 2 and 3). PARP-1 automodification (self-PARylation) is accompanied by formation of an intermediate complex, and eventually leads to nearly complete recovery of the initial structure of nucleosome (Figure 4). Thus spFRET is a sensitive method for analysis of PARP-1-induced changes in chromatin structure that could also be used for analysis of PARP-1 inhibition by various compounds.

PARP-1 binds to nucleosomes having one linker DNA with an exposed double-strand break with stoichiometry of one PARP-1 molecule per nucleosome [12]. Rearrangements in the enzyme structure after binding to a double-strand DNA break [7] make HD subdomain unstable, resulting in activation of the catalytic center of PARP-1 [26,27]. If PARP-1 is bound in the vicinity of a nucleosome, activated PARP-1 can also induce a considerable, partial and reversible disturbance of nucleosomal DNA structure (Figure 5). Similar, although less pronounced changes of nucleosomal structure have been observed after acetylation of core histones and DNA methylation in a nucleosome [28,29]. Much more dramatic uncoiling of nucleosomal DNA together with the associated core histones was observed in the complex between yFACT and a nucleosome [16]. It is possible that yFACT and PARP-1 induce conformational changes in nucleosomal DNA of similar nature, but different magnitude.

Nucleosome structure can be considerably changed during various processes, such as transcription [30-32] and protein binding to nucleosomal DNA [33]. These conformational changes include: (i) DNA unwrapping from an intact octamer; (ii) DNA unwrapping accompanied by opening of the (H2A-H2B) dimer/(H3-H4)₂ tetramer interface; (iii) DNA unwrapping with complete octamer disassembly and (iv) the unwrapping involving opening of the (H3-H4)₂ tetramer [34-36]. Since different regions of nucleosomal DNA are uncoiled in the PARP-1-nucleosome complex to a similar degree (Figure 5), the global change in the nucleosome structure involving structural changes in the entire histone octamer likely occurs. The nature and extent of these conformational changes in nucleosome structure remain to be determined.

Detection and repair of double-strand breaks in cells require multi-step chromatin remodeling. Thus p400/Tip60 chromatin remodeler induces exchange of histones H2A to H2A.Z onto nucleosomes at the break, which is important for downstream acetylation of H4 histone and maintenance of less compact chromatin structure in the break region [37]. PARP-1-induced DNA uncoiling could facilitate the histone exchange and/or displacement during the chromatin remodeling, before PARP-1 leaves the DNA break after automodification. It is also possible that the stable PARP-1-nucleosome complexes could be formed at transcription start sites [4].

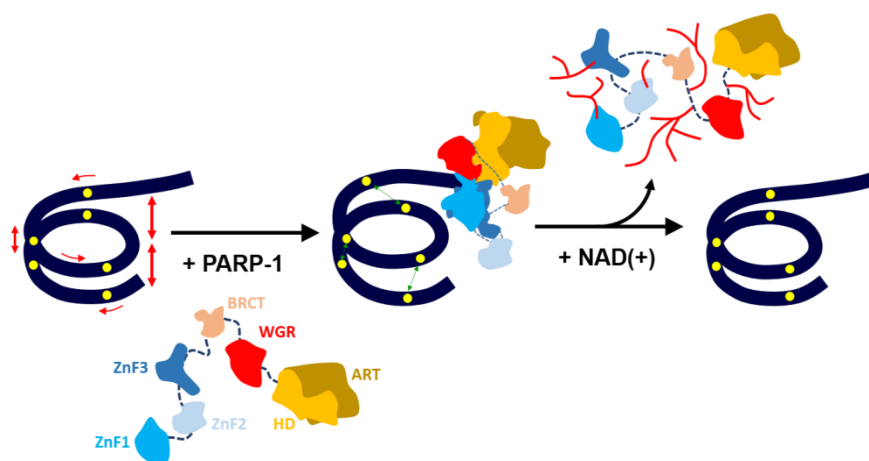


Figure 5. The model of PARP-1-induced conformational changes in nucleosomal DNA in the vicinity of double-strand DNA break. DNA is tightly wrapped around histone octamer, but there are fluctuations in the structure of the double helix, especially in an area near DNA entering or exiting the nucleosome core. Unmodified PARP-1 is inactive and its domains (shown by different colors) are connected together by flexible linkers [26]. When PARP-1 binds to a DNA damage or available DNA end in the vicinity of a nucleosome, it forms a compact structure [7], which induces activation of PARP-1 and partial unwrapping of nucleosomal DNA. This nucleosome unfolding is accompanied by a reduced mobilities of the +13, +35 and +112 regions of nucleosomal DNA and possibly by destabilization of the intranucleosomal interactions between core histones. In the presence of NAD^+ PARP-1 is automodified and released from the nucleosome; PARP-1 release is accompanied by spontaneous recoiling of nucleosomal DNA. Yellow circles indicate positions of the pairs of fluorescent dyes on nucleosomal DNA.

5. Conclusions

Nucleosome structure can be considerably and reversibly unfolded after PARP-1 binding. These changes include transient and partial uncoiling of nucleosomal DNA along its entire length. These PARP-1-dependent changes in nucleosome structure are nearly completely reversed after PARP-1 eviction due to its auto-poly(ADP)-ribosylation.

Acknowledgments

We thank Daria Gaykalova for help with designing the fluorescent probes. This work was supported by NIH grants GM58650 to V.M.S. and GM087282 to J.M.P., and by the Federal Target Program “Research and developments in the priority directions of the scientific-technological complex of the Russian Federation for 2014–2020” (Agreement of the Ministry of Education of the Russian Federation No 14.604.21.0063, RFMEFI60414X0063).

Conflict of interest

The authors declare no competing financial interests.

References

1. Beard BC, Wilson SH, Smerdon MJ (2003) Suppressed catalytic activity of base excision repair enzymes on rotationally positioned uracil in nucleosomes. *Proc Natl Acad Sci U S A* 100: 7465-7470.
2. Caldecott KW (2007) Mammalian single-strand break repair: mechanisms and links with chromatin. *DNA Repair (Amst)* 6: 443-453.
3. De Vos M, Schreiber V, Dantzer F (2012) The diverse roles and clinical relevance of PARPs in DNA damage repair: current state of the art. *Biochem Pharmacol* 84: 137-146.
4. Kraus WL (2008) Transcriptional control by PARP-1: chromatin modulation, enhancer-binding, coregulation, and insulation. *Curr Opin Cell Biol* 20: 294-302.
5. Ali AA, Timinszky G, Arribas-Bosacoma R, et al. (2012) The zinc-finger domains of PARP1 cooperate to recognize DNA strand breaks. *Nat Struct Mol Biol* 19: 685-692.
6. Eustermann S, Wu WF, Langelier MF, et al. (2015) Structural Basis of Detection and Signaling of DNA Single-Strand Breaks by Human PARP-1. *Mol Cell* 60: 742-754.
7. Langelier MF, Planck JL, Roy S, et al. (2012) Structural basis for DNA damage-dependent poly(ADP-ribosylation) by human PARP-1. *Science* 336: 728-732.
8. Martinez-Zamudio R, Ha HC (2012) Histone ADP-ribosylation facilitates gene transcription by directly remodeling nucleosomes. *Mol Cell Biol* 32: 2490-2502.
9. Tanuma S, Kawashima K, Endo H (1985) Comparison of ADP-ribosylation of chromosomal proteins between intact and broken cells. *Biochem Biophys Res Commun* 127: 896-902.
10. Gunderson CC, Moore KN (2015) Olaparib: an oral PARP-1 and PARP-2 inhibitor with promising activity in ovarian cancer. *Future Oncol* 11: 747-757.
11. Fong PC, Boss DS, Yap TA, et al. (2009) Inhibition of poly(ADP-ribose) polymerase in tumors from BRCA mutation carriers. *N Engl J Med* 361: 123-134.
12. Clark NJ, Kramer M, Muthurajan UM, et al. (2012) Alternative modes of binding of poly(ADP-ribose) polymerase 1 to free DNA and nucleosomes. *J Biol Chem* 287: 32430-32439.
13. Kudryashova KS, Chertkov OV, Nikitin DV, et al. (2015) Preparation of Mononucleosomal Templates for Analysis of Transcription with RNA Polymerase Using spFRET. *Methods Mol Biol* 1288: 395-412.
14. Chertkov OV, Studitsky VM, Feofanov AV, et al. (2016) Change in conformation of linker DNA upon binding of histone H1.5 to nucleosome: fluorescent microscopy of single complexes. *Mosc Univ Biol Sci Bull* 71: 108-113.
15. Feofanov AV, Kudryashova KS, Chertkov OV, et al. (2015) Analysis of nucleosome transcription using single-particle FRET. *Springer Proc Phys* 164: 255-260.
16. Valieva ME, Armeev GA, Kudryashova KS, et al. (2016) Large-Scale ATP-Independent Nucleosome Unfolding by a Histone Chaperone. *Nat Struct Mol Biol*: In press.
17. Langelier MF, Planck JL, Servent KM, et al. (2011) Purification of human PARP-1 and PARP-1 domains from *Escherichia coli* for structural and biochemical analysis. *Methods Mol Biol* 780: 209-226.
18. Kulaeva OI, Gaykalova DA, Pestov NA, et al. (2009) Mechanism of chromatin remodeling and recovery during passage of RNA polymerase II. *Nat Struct Mol Biol* 16: 1272-1278.
19. Kireeva ML, Walter W, Tchernajenko V, et al. (2002) Nucleosome remodeling induced by RNA polymerase II: loss of the H2A/H2B dimer during transcription. *Mol Cell* 9: 541-552.

20. Studitsky VM, Clark DJ, Felsenfeld G (1995) Overcoming a nucleosomal barrier to transcription. *Cell* 83: 19-27.
21. Vasudevan D, Chua EY, Davey CA (2010) Crystal structures of nucleosome core particles containing the '601' strong positioning sequence. *J Mol Biol* 403: 1-10.
22. Thastrom A, Lowary PT, Widlund HR, et al. (1999) Sequence motifs and free energies of selected natural and non-natural nucleosome positioning DNA sequences. *J Mol Biol* 288: 213-229.
23. Muthurajan UM, Hepler MR, Hieb AR, et al. (2014) Automodification switches PARP-1 function from chromatin architectural protein to histone chaperone. *Proc Natl Acad Sci U S A* 111: 12752-12757.
24. Zahradka P, Ebisuzaki K (1982) A shuttle mechanism for DNA-protein interactions. The regulation of poly(ADP-ribose) polymerase. *Eur J Biochem* 127: 579-585.
25. Ogata N, Ueda K, Kawaichi M, et al. (1981) Poly(ADP-ribose) synthetase, a main acceptor of poly(ADP-ribose) in isolated nuclei. *J Biol Chem* 256: 4135-4137.
26. Steffen JD, McCauley MM, Pascal JM (2016) Fluorescent sensors of PARP-1 structural dynamics and allosteric regulation in response to DNA damage. *Nucleic Acids Res*: gkw710.
27. Dawicki-McKenna JM, Langelier MF, DeNizio JE, et al. (2015) PARP-1 Activation Requires Local Unfolding of an Autoinhibitory Domain. *Mol Cell* 60: 755-768.
28. Lee JY, Lee TH (2012) Effects of DNA methylation on the structure of nucleosomes. *J Am Chem Soc* 134: 173-175.
29. Lee JY, Wei S, Lee TH (2011) Effects of histone acetylation by Piccolo NuA4 on the structure of a nucleosome and the interactions between two nucleosomes. *J Biol Chem* 286: 11099-11109.
30. Chang HW, Shaytan AK, Hsieh FK, et al. (2013) Structural Analysis of the Key Intermediate Formed during Transcription through a Nucleosome. *Trends Cell Mol Biol* 8: 13-23.
31. Pestov NA, Gerasimova NS, Kulaeva OI, et al. (2015) Structure of transcribed chromatin is a sensor of DNA damage. *Sci Adv* 1: e1500021.
32. Gaykalova DA, Kulaeva OI, Volokh O, et al. (2015) Structural analysis of nucleosomal barrier to transcription. *Proc Natl Acad Sci U S A* 112: E5787-5795.
33. Zaret KS, Carroll JS (2011) Pioneer transcription factors: establishing competence for gene expression. *Genes Dev* 25: 2227-2241.
34. Bohm V, Hieb AR, Andrews AJ, et al. (2011) Nucleosome accessibility governed by the dimer/tetramer interface. *Nucleic Acids Res* 39: 3093-3102.
35. Tomschik M, Zheng H, van Holde K, et al. (2005) Fast, long-range, reversible conformational fluctuations in nucleosomes revealed by single-pair fluorescence resonance energy transfer. *Proc Natl Acad Sci U S A* 102: 3278-3283.
36. Zlatanova J, Bishop TC, Victor JM, et al. (2009) The nucleosome family: dynamic and growing. *Structure* 17: 160-171.
37. Xu Y, Ayrapetov MK, Xu C, et al. (2012) Histone H2A.Z controls a critical chromatin remodeling step required for DNA double-strand break repair. *Mol Cell* 48: 723-733.

